Chemical Methodologies 6(2022) 331-338

Chemical Methodologies

Journal homepage: http://chemmethod.com

Original Research Article

Acid Activation of Iraqi Bentonite Clay: Its Structural, Dielectric and Electrical Behavior at Various Temperatures

Ali Jabbar Al-Saray[1,*], Israa Mohamed H. Al-Mousawi[1], Taghreed H. Al-Noor[2]

[1]*Department of Chemistry, College of Science, University of Baghdad, Baghdad, Iraq*
[2]*Department of Chemistry, College of Education for pure sciences Ibn-Alhaitham, University of Baghdad, Baghdad, Iraq*

ARTICLE INFO

Article history

Submitted: 2022-02-07
Revised: 2022-02-12
Accepted: 2022-03-04
Manuscript ID: CHEMM-2202-1439
Checked for Plagiarism: **Yes**
Language Editor:
Dr. Behrouz Jamalvandi
Editor who approved publication:
Dr. Sami Sajjadifar

DOI:10.22034/CHEMM.2022.328714.1439

KEYWORDS

Bentonite
Dielectric constant
Conductivity
Impedance
Permittivity
Tangent loss factor

ABSTRACT

Iraqi calcium bentonite was activated via acidification to study its structural and electrical properties. The elemental analysis of treated bentonite was determined by using X-ray fluorescence while the unit crystal structure was studied through X-ray diffraction showing disappearance of some fundamental reflections due to the treatment processes. The surface morphology, on the other hand, was studied thoroughly by Scanning Electron microscopy SEM and Atomic Force Microscope AFM showing some fragments of montmorillonite sheets. Furthermore, the electrical properties of bentonite were studied including: The dielectric permittivity, conductivity, tangent loss factor, and impedance with range of frequency (0.1-1000 KHz) at different temperatures.

GRAPHICAL ABSTRACT

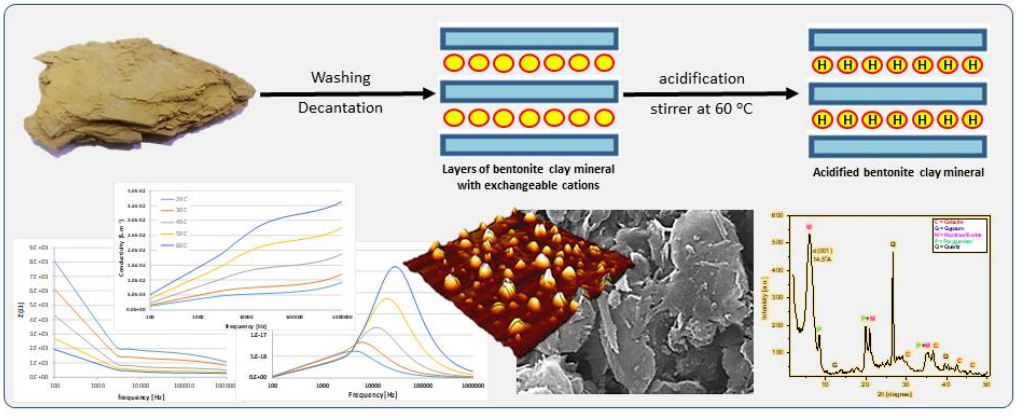

* Corresponding author: Ali J. Al-Saray
✉ E-mail: albaghdady1993@gmail.com

Introduction

Recently, the need for clean alternative and environment friendly materials is growing rapidly, specifically for materials, having the ability to store electricity such as electrochemical super capacitors or ultra-capacitors or others, which can be charged and discharged rapidly, as well as materials with different electrical behavior with respect to the temperature and the frequency of applied field [1].

Bentonite is considered as a clay mineral which belonging to the semantic clays and contains mineral montmorillonite and aluminum hydro silicate [2]. The composition of bentonite includes mainly silicon dioxide and less fraction of aluminum oxide [3], where the crystal structure of montmorillonite consists of an octahedral sheet of aluminum hydr(oxides) sited between two tetrahedral sheets of SiO4 [2].

Bentonite is a widespread, environmental friendly, economical and easily available material as its structural layers contain a large number of mesoporous, which can be used as a catalyst due to its interaction capability with metals and other materials as well as being used for preparing polymeric composites as an inorganic filler that possess high conductivity [4,5]. The increasing application of clay minerals specially in the process of manufacturing advanced materials raises the necessity for enrichment and purification.

It is worth noting that measuring charge carrying and other electrical properties of isolated materials gains a great attention lately, because it can provide information about electronic structure of these materials as well as the mechanism of conductance as a response to the applied field. Hence, more studies have been conducted and more models have been designed to explain the mechanisms of electrical behavior. Consequently, there are two types of charge carriers, namely electrons and ions; additionally, there are different mechanisms for the charge carriers to move inside the isolators under the applied field. These isolators can be used in a lot of electrical system whether on the microelectronic scale or the overhead power scale [6].

Material and Methods

Calcium bentonite clay with chemical formula [Ca $(Al,Fe,Zn)_2$ $(Al,Si)_4O_{10}(OH)_2$ nH_2O] and chemical composition was supplied from the Ministry of Industry and Minerals-Iraqi Geological Survey as shown in

Table 1. The raw bentonite was crashed to powder form in order to be ready for decantation process where most of the silica was separated from the bentonite. After that, bentonite was washed repeatedly with excessive amount of distilled water to remove excess salts as well as separate undesired soluble impurities (Figure 1).

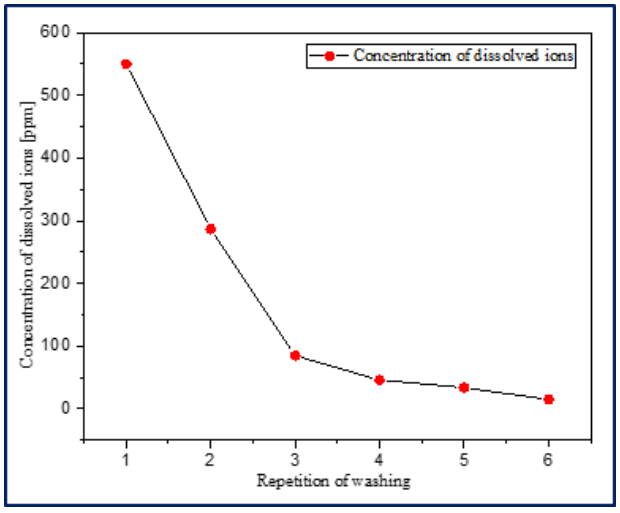

Figure 1: Conc. of total dissolved ions in bentonite with respect to the repetition of washing

Acid treatment was conducted to bentonite in an attempt to remove some of the insoluble species such as calcium carbonate present in form of calcite. 10 gm of bentonite powder was dispersed in 100 ml of 0.10 N hydrochloric acid solution followed by heating to 60 oC with stirring for two hours and then left to cool down at room temperature overnight [7].

However, high acidity of bentonite is not desirable [8]; thus, the suspended solution of bentonite was washed strongly with deionized water using Soxhlet apparatus for 24 hours, so as to mitigate and get rid of the percussions of acidity. Moreover, after being washed, the treated clay was dried at 80 oC for two hours followed by grinding in order to be characterized and studied.

Table 1: Chemical composition of Iraqi calcium bentonite

Oxides	MgO	Al_2O_3	CaO	SiO_2	Fe_2O_3	K_2O	MnO	TiO_2	L.O.I.	Total
% Wt.	3.20	13.30	5.70	57.20	6.10	1.09	0.02	0.80	12.00	99.41
% Wt.*	3.70	15.36	6.58	66.06	7.04	1.26	-	-	-	100

* : % Weights after deduction of LOI, TiO_2, and MnO

On the other hand, the electrical measurements were conducted by using HIOKI IM3534 high frequency impedance analyzer (4294 A) with range of frequency (0.1 KHz- 1 MHz) and 0.05% accuracy. Furthermore, the dielectric permittivity and tangent loss factor were estimated through using the following equations [9]:

$$\varepsilon' = \varepsilon_\infty + \frac{\Delta\varepsilon}{1+\omega^2\tau^2}$$

$$\varepsilon'' = \frac{\Delta\varepsilon\ \omega\tau}{1+\omega^2\tau^2}$$

$$tan\delta = \varepsilon''/\varepsilon'$$

Where ε^' is the real component of dielectric permittivity, ε^'' is the imaginary component dielectric permittivity, ε_∞ is the infinite permittivity, ω is field frequency, tanδ is the tangent loss factor, and τ is the relaxation time.

Results and Discussion

X-ray diffraction analysis

The structure of bentonite was characterized through studying its X-ray diffraction diagram; where (figure 2) illustrates bentonite's X-ray diffraction which contains the main known reflections of bentonite clay except for two peaks usually located at 29 and 11-13 (2θ), which belong to calcite and gypsum respectively due to treatment processes [10]. The reflection observed at 6.1 (2θ) is a characteristic d(001) peak for montmorillonite, while other main reflection can be noticed at 26.7 (2θ), which is the characteristic reflections of quartz. Polygarsket reflection, on the other hand, appears at 8.5 (2θ) [11].

Further, the interplanar spacing between the bentonite layers were estimated via using Bragg's law, while the average particle sizes were estimated using the data from the reflections in diffractograms and employing Debye-Scherer relation [12]. The values of d-spacing, FWHM, and the crystalline size are tabulated in Table 2.

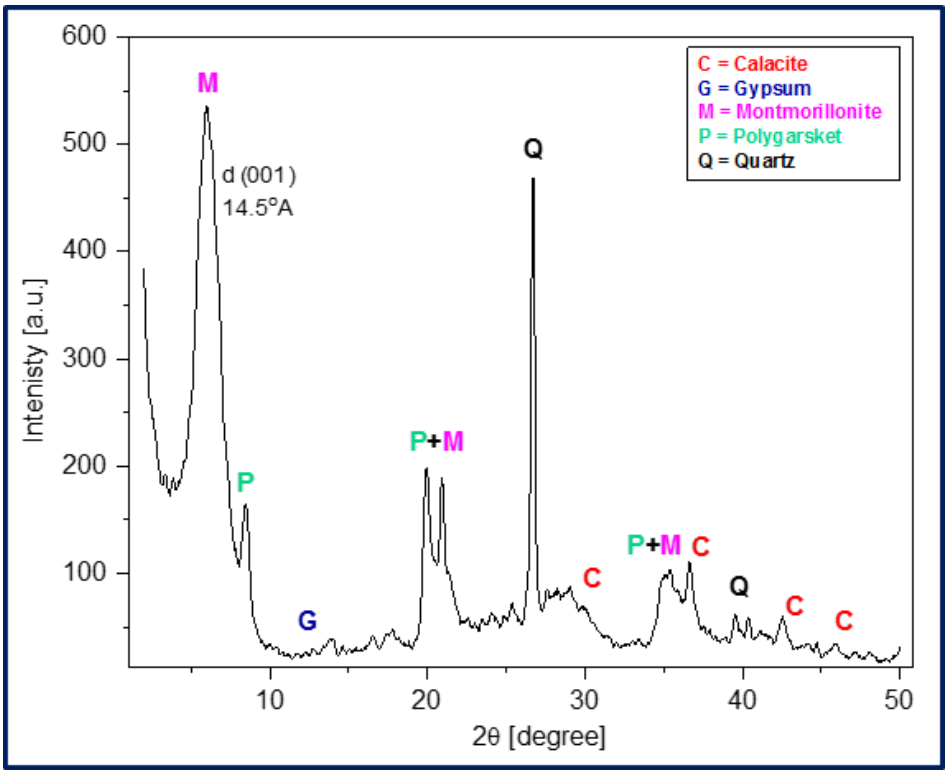

Figure 2: X-ray diffractogram of treated Ca-bentonite

Table 2: values of Intensities, d-spacing, FWHM, and crystalline size of the treated Ca-bentonite

Peak number	2θ	Intensity [a.u.]	d-spacing [A°]	FWHM [deg.]	$D_{Average}$ (nm)
1	6.104	219	14.467	0.3916	29.020
2	8.613	66	10.259	0.3546	
3	20.611	42	4.306	0.4368	
4	20.957	123	4.236	0.2341	
5	25.324	19	3.514	0.1164	
6	26.729	415	3.333	0.1775	
7	35.138	31	2.552	0.2858	
8	36.674	43	2.448	0.3250	

Morphological analysis

The SEM images of treated bentonite are depicted in (Figure 3), where the particles appeared with irregularly spherical geometry due to the stacking sheets of clay compositions. However, some sheet fragments appeared in 1-5 µm scale images, which can be attributed to some exfoliated montmorillonite layers, which are most likely to be in the nano-scale. On the other hand, the three-dimensional atomic force microscopic images show certain arranging pattern for clay particles, which can be taken as an evidence for formation of nano-scale particles as depicted in Figure 4.

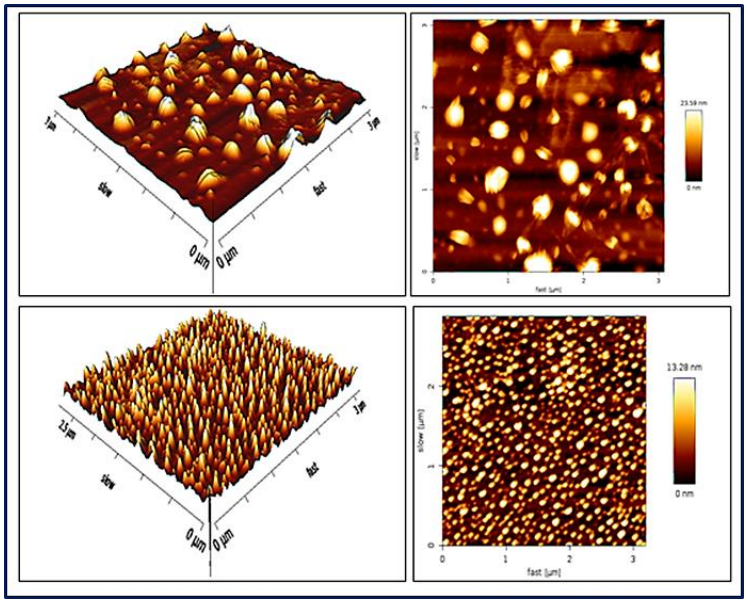

Figure 3: AFM surface images of treated Ca-bentonite

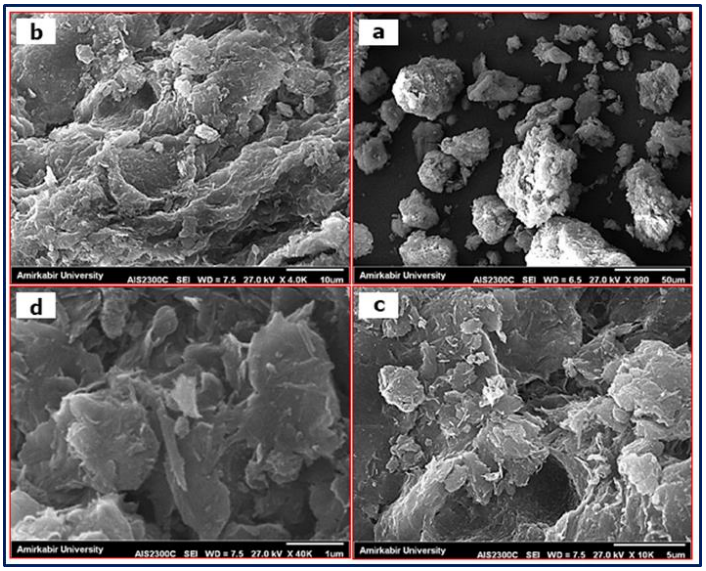

Figure 4: SEM images of treated Ca-bentonite at scale of (a) 50 µm, (b) 10 µm, (c) 5 µm, and (d) 1 µm

Dielectric permittivity

The real component of dielectric permittivity spectrum of Ca-bentonite (Figure 5) at low frequency region in the range (0.1-10 KHz) shows constant behavior at variant temperatures, which indicates that the slow motion of the applied field is insufficient to liberate the charge carriers from its restricted force field [13]. However, the dielectric breakdown has occurred at different frequency according to variant temperatures. At low temperatures (24-30) °C, the breakdown starts at approximately 5 KHz where charge carriers are easily oriented with the applied field due to low thermal kinetic energies. Otherwise, the breakdown of higher temperatures (40-60 °C) takes place at much higher frequencies (10-40 KHz).

On the other hand, at (100-1000 KHz) frequencies, the behavior has linear trend similar to the low frequency region indicating the state of stability for the charge carriers with respect to the applied field. Moreover, as much as the temperature increases, the beginning of stability state shifts to higher frequencies [14].

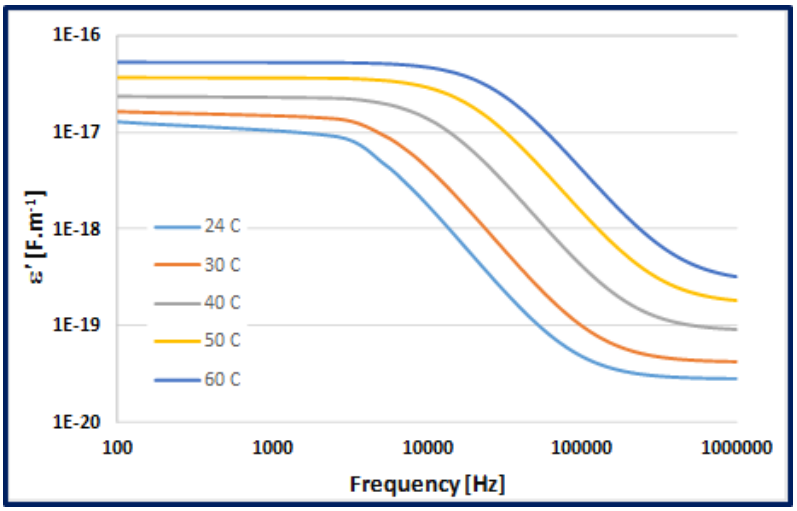

Figure 5: The real dielectric permittivity spectrum of the treated Ca-bentonite

The imaginary part of the dielectric permittivity of Ca-bentonite provides information regarding the loss of energies. The peaks in Figure 6 located in range of frequency (5-100 KHz) represent the energy losses as a result of the maximum response of charge carrier movement with the applied field. Furthermore, the maximum responses are shifted to higher frequencies as well as higher intensities with respect to increasing the temperature due to the increase in random movement of charge carrier as the temperature elevated.

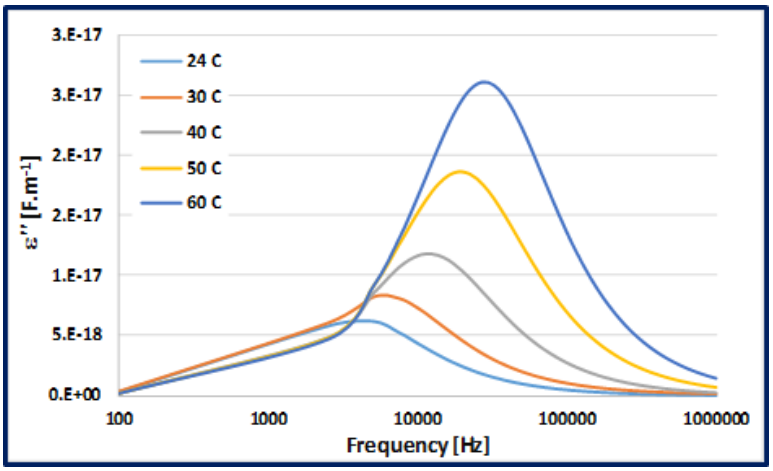

Figure 6: The imaginary dielectric permittivity spectrum of the treated Ca-bentonite

Tangent loss factor

The tangent loss factor "tan(δ)" spectrum for Ca-bentonite shows regions of resonance with the applied field (Figure 7) as bands with maximum values of energy losses. These bands are shifted with increasing the temperature to the higher frequencies due to increasing the randomized kinetic energies, which have been added to the

charge carriers. Thus, the motions of charge carriers harmonize with higher frequencies with respect to increasing temperature. On the other hand, increasing the intensity of the peaks is noticed with increasing temperature, which can be attributed the response of charge carrier in Ca-bentonite with the applied field.

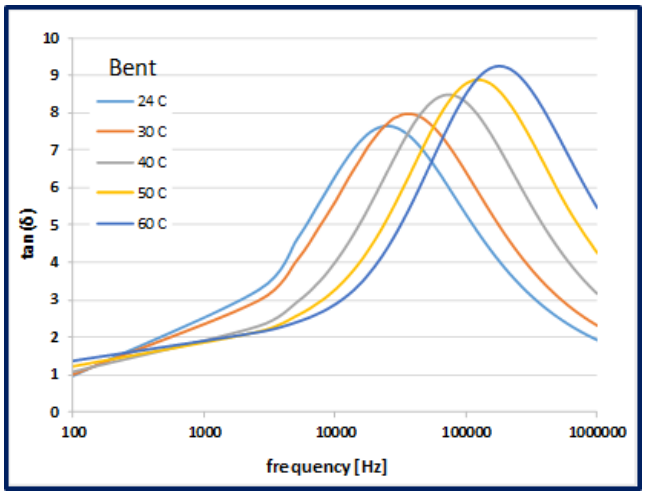

Figure 7: Tangent loss factor spectrum of the treated Ca-bentonite

Electrical conductivity

Bentonite conductivity spectrum (Figure 8) shows no significant variance in conductivity with different frequencies of the applied field at low temperatures especially 24-30 °C. The reason could be attributed to the presence of the charge carriers in the ground energy state, which cannot be responding considerably to the applied field changes [15]. Whereas in the (40-60) range of temperatures where the conductivities are increasing noticeably with the field.

High temperatures provide more kinetic energies to the charge carriers in order to exceed the energy barrier, thus responding to the applied field. Furthermore, the slope of the conductivity lines increases as the temperature gets higher with respect to the increasing of the frequency of the applied field.

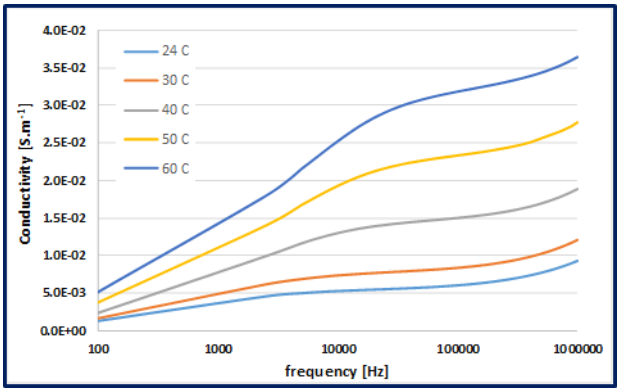

Figure 8: conductivity spectrum of the treated Ca-bentonite

Electrical impedance

A typical impedance behavior of treated Ca-bentonite has been noticed (Figure 9) where the impedance decreases with increasing both temperature and the applied field frequencies. The effect of increasing the temperature can be attributed to increasing of the kinetic energy of charge carriers as carrying the electric current is increasing accordingly [16].

However, the effect of increasing the frequency is quite different, a steep drop in the impedance in range of (0.1-5.1 KHz), which indicates a high and quick response of the charge carriers with respect to the increasing frequency leading to a resonance and harmony between the charge carriers and the applied field in that range of frequencies. On the other hand, the decreasing of impedance appeases to be significantly less steep at high frequency region.

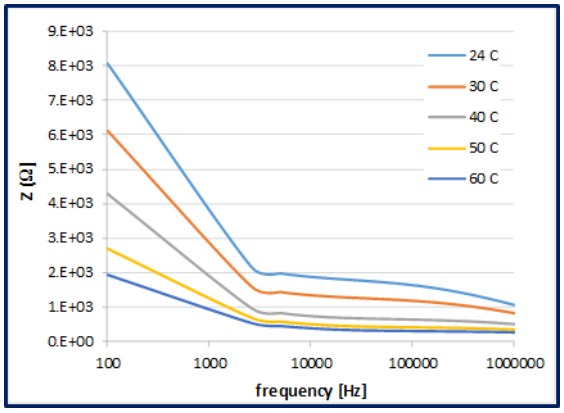

Figure 9: Impedance spectrum of the treated Ca-bentonite

Conclusion

Activation of Iraqi bentonite clay led to some structural and compositional changes according to X-ray diffraction. The morphology of bentonite surface AFM shows formation of nano-scale particles which agreed with the SEM images where sheets of montmorillonite were noticed. At low temperature bentonite exhibits almost a constant and low conductivity behavior as well as very high impedance as there is less loss of energy of the field. However, when the temperature increases, both the conductivity and the loss of energy of the field increases accordingly with very low impedance behavior. Permittivity spectrum, on the other hand, shows a behavior which agrees with the other electrical measurement, as it increases with increasing temperatures due to the higher thermal energy.

Acknowledgments

The authors would like to express their gratitude and thanks to the research opportunity given by University of Baghdad for providing the materials and lab facilities.

Funding

This research did not receive any specific grant from fundig agencies in the public, commercial, or not-for-profit sectors.

Authors' contributions

All authors contributed toward data analysis, drafting and revising the paper and agreed to responsible for all the aspects of this work.

Conflict of Interest

We have no conflicts of interest to disclose.

ORCID

Ali Jabbar A. Al-Sarray
https://www.orcid.org/0000-0001-6484-1763
Israa Mohamed H. Al-Mousawi
https://www.orcid.org/0000-0003-1067-6939
Taghreed H. Al-Noor
https://www.orcid.org/0000-0002-6761-7131

References

[1]. Conway B.E., Pell W.G., *J. Solid State Electrochem.*, 2003, **7**:637 [Crossref], [Google Scholar], [Publisher]

[2]. Saltas V., Vallianatos F., Triantis D., *J. Non-Cryst. Solids*, 2008, **354**:5533 [Crossref], [Google Scholar], [Publisher]

[3]. Jiang Y.X., Xu H.J., Liang D.W., Tong Z.F., *C. R. Chim.*, 2008, **11**:125 [Crossref], [Google Scholar], [Publisher]

[4]. Jeenpadiphat S., Tungasmita D.N., *Appl. Clay Sci.*, 2014, **87**:272 [Crossref], [Google Scholar], [Publisher]

[5]. Sang S., Zhang J., Wu Q., Liao Y., *Electrochim. Acta*, 2007, **52**:7315 [Crossref], [Google Scholar], [Publisher]

[6]. Tjong S.C., Mai Y.W., Elsevier, 2010 [Google Scholar]

[7]. Temuujin J., Senna M., Jadambaa T., Burmaa D., Erdenechimeg S., MacKenzie K.J., *J. Chem. Technol. Biotechnol.: Int. Res. Process, Environ. Clean Technol.*, 2006, **81**:688 [Crossref], [Google Scholar], [Publisher]

[8]. Mokaya R., Jones W., Davies M.E., Whittle M.E., *J. Solid State Chemistry.*, 1994, **111**:157 [Crossref], [Google Scholar], [Publisher]

[9]. Madakbas S., Esmer K., Kayahan E., Yumak M., *Sci. Eng. Compos. Mater.*, 2010, **17**:145 [Crossref], [Google Scholar], [Publisher]

[10]. Foletto E.L., Volzone C., Porto L.M., *Lat. Am. Appl. Res.*, 2006. **36**:37 [Google Scholar], [Publisher]
[11]. Tabak A., Afsin B., Caglar B.Ü.L.E.N.T., Koksal E.K.R.E.M., *J. Colloid Interface Sci.*, 2007, **313**:5 [Crossref], [Google Scholar], [Publisher]
[12]. Seeck O.H., Murphy B., *X-ray diffraction: Modern experimental techniques*. 2015: CRC Press [Google Scholar], [Publisher]
[13]. Coşkun, M., Polat Ö., Coşkun F.M., Durmuş Z., Çağlar M., Türüt A.B.D.U.L.M.E.C.İ.T., *RSC Adv.*, 2018, **8**:4634 [Crossref], [Google Scholar], [Publisher]
[14]. Mariappan C.R., Govindaraj G., Rathan S.V., Prakash G.V., *Mater. Sci. Eng.: B*, 2005, **121**:2 [Crossref], [Google Scholar], [Publisher]
[15]. Pradhan D.K., Choudhary R.N.P., Samantaray B.K., Thakur A.K., Katiyar R.S., *Ionics*, 2009, **15**:345 [Crossref], [Google Scholar], [Publisher]
[16]. Joshi J.H., Kanchan D.K., Joshi M.J., Jethva H.O., Parikh K.D., *Mater. Res. Bull.*, 2017, **93**:63 [Crossref], [Google Scholar], [Publisher]

HOW TO CITE THIS ARTICLE
Ali J. Al-Saray, Israa M. Al-Mussawi, Taghreed H. Al-Noor. Acid Activation of Iraqi Bentonite Clay and Studying its Structural, Dielectric and Electrical Behavior at Various Temperatures. *Chem. Methodol.*, 2022, 6(4) 331-338
https://doi.org/10.22034/CHEMM.2022.328714.1439
URL: http://www.chemmethod.com/article_146442.html